The Single-Ring Thermoanaerobacter brockii Chaperonin 60 (Tbr-EL7) Dimerizes to Tbr-EL14.cntdot.Tbr-ES7 under Protein Folding Conditions

ARTICLE *in* BIOCHEMISTRY · NOVEMBER 1995

Impact Factor: 3.02 · DOI: 10.1021/bi00045a038 · Source: PubMed

5 AUTHORS, INCLUDING:

Matthew J Todd
Johnson & Johnson
47 PUBLICATIONS **2,897** CITATIONS
SEE PROFILE

George Lorimer
University of Maryland, College Park
137 PUBLICATIONS **9,575** CITATIONS
SEE PROFILE

The Single-Ring *Thermoanaerobacter brockii* Chaperonin 60 (*Tbr*-EL_7) Dimerizes to *Tbr*-EL_{14}•*Tbr*-ES_7 under Protein Folding Conditions

Matthew J. Todd,*,‡ Stefan Walke,§ George Lorimer,‡ Kaye Truscott,|| and Robert K. Scopes||

Central Research & Development Department, Experimental Station, DuPont Co., Wilmington, Delaware 19880-0402, Institut fur Biophysik und Physikalische Biochemie, Universitat Regensburg, Universitatsstrasse 31, 8400 Regensburg, Germany, and Centre for Protein and Enzyme Technology and School of Biochemistry, LaTrobe University, Bundoora, Victoria 3083, Australia

Received May 31, 1995; Revised Manuscript Received September 7, 1995®

ABSTRACT: Chaperone proteins assist in the folding of some newly synthesized proteins and inhibit protein aggregation. The *Thermoanaerobacter brockii* chaperonin proteins (*Tbr*-EL and *Tbr*-ES) have recently been purified and characterized [Truscott, W. N., Høj, P. B., & Scopes, R. K. (1994) *Eur. J. Biochem. 222*, 277−284]; *Tbr*-EL was a single seven-membered toroid, unlike most GroELs which exist as double toroids. Using high-resolution gel filtration chromatography, we have resolved the purified *Tbr*-EL into single ringed (*Tbr*-EL_7) and double ringed (*Tbr*-EL_{14}) species. The latter contained tightly bound *Tbr*-ES co-chaperonin (*Tbr*-EL_{14}•*Tbr*-ES_7). In the presence of Mg•ATP and either *Escherichia coli* GroES (*Eco*-ES) or *Tbr*-ES (i.e., under protein folding conditions), the isolated Tbr-EL_7 rapidly dimerized to the *Tbr*-EL_{14}•*Eco*-ES_7 or *Tbr*-EL_{14}•*Tbr*-ES_7 complexes. The doubly toroidal species thus formed contained ≥ 6 molecules tightly bound ADP and one $GroES_7$ and are similar to the asymmetric chaperonin complex isolated from *Thermus thermophilus* [Taguchi, H., Konishi, J., Ishii, N., & Yoshida, M. (1991) *J. Biol. Chem. 266*, 22411−22418]. The isolated *Tbr*-EL_7 and *Tbr*-EL_{14}•*Tbr*-ES_7 hydrolyzed ATP at ~2 and 1 min^{-1}, respectively. Addition of a molar excess of *Eco*-ES_7 to the isolated *Tbr*-EL_7 reduced the ATPase activity to 1 min^{-1}, consistent with the formation of *Tbr*-EL_{14}•*Eco*-ES_7. *Eco*-ES_7 failed to inhibit the *Tbr*-EL_{14}•*Tbr*-ES_7 complex. The isolated *Tbr*-EL_{14}•*Tbr*-ES_7 complex did not support the folding of Rubisco under nonpermissive conditions. Only when the complex was supplemented with additional GroES was folding of Rubisco observed; i.e., one molar equivalent of GroES was not sufficient for folding. Both *Tbr*-EL_7 and *Tbr*-EL_{14}•*Tbr*-ES_7 bound one unfolded [^{35}S] *Rhodospirillum rubrum* Rubisco per mole particle. In contrast, *Eco*-EL_{14} bound 2 mol of protein per mole particle, consistent with each toroid having a peptide binding site. *Eco*-EL_{14}•*Eco*-ES_7 complex only bound one unfolded protein, thus GroES binding blocks one GroEL peptide binding site. Addition of *Eco*-ES_7 to a *Eco*-EL_{14}•$Rubisco_2$ complex did not result in the displacement of one molecule of Rubisco but in the formation of a ternary *Eco*-EL_{14}•$Rubisco_2$•*Eco*-ES_7 complex.

Chaperonin proteins both facilitate the folding of some other proteins (Goloubinoff et al., 1989) and prevent the aggregation of nonnative proteins (Buchner et al., 1991). The complete chaperonin system consists of two heptameric, toroidal proteins, GroEL[1] (protomer mass about 60 kDa) and GroES (protomer mass about 10 kDa). The latter is necessary when the conditions for spontaneous protein folding are nonpermissive (Schmidt et al., 1994a). The toroidal structure is thought to be essential to chaperonin function; unfolded proteins are thought to interact with the hydrophobic surface facing the central cavity (Braig et al., 1994; Langer et al., 1992; Chen et al., 1994). Most members of the GroEL family, including that from the thermophilic bacterium *Thermus thermophilus* (Taguchi et al., 1991), exist as 14-mers, doubly toroidal structures (Hendrix, 1979; McMullin & Hallberg, 1988; Pushkin et al., 1982). The mechanism for GroEL-assisted folding is thought to involve alternating states of high and low affinity for unfolded proteins. ATP hydrolysis drives the interconversion between these ill-defined states, causing release of unfolded proteins, and allowing them a chance to fold free in solution (Todd et al., 1994; Weissman et al., 1994). A recently proposed mechanism for the GroEL reaction cycle incorporated these high and low affinity states into a model which included a symmetric intermediate, with *two* GroES molecules transiently bound (Todd et al., 1994). With each turnover, the tightly bound GroES and ADP were released. The function of GroES was proposed to "quantize" ATP hydrolysis on the GroEL toroid which was unligated, supplying sufficient

* To whom correspondence should be addressed. Phone: 302-695-9748. Fax: 302-695-4509.
‡ DuPont Co.
§ Universitat Regensburg.
|| LaTrobe University.
® Abstract published in *Advance ACS Abstracts,* November 1, 1995.
[1] Abbreviations: To prevent possible confusion when analyzing characteristic of chaperonins from different sources, we use the following nomenclature (borrowed from that used to identify restriction enzymes) to indicate the origin of each species: *Thermoanaerobacter brockii* chaperonin proteins GroEL and GroES: *Tbr*-EL, *Tbr*-ES; *Thermus thermophilus* GroEL and GroES: *Tth*-EL, *Tth*-ES; *Escherichia coli* GroEL and GroES: *Eco*-EL, *Eco*-ES. Subscripts refer to the number of subunits in each particle. Other abbreviations: ATP, adenosine triphosphate; ADP, adenosine diphosphate; AMP-PNP, 5′-adenylylimidodiphosphate; ATP-γ-S, adenosine 5′-*O*-(3-thiotriphosphate); DTT, DL-dithiothreitol; EDTA, ethylenediaminetetraacetic acid; Rubisco, ribulose-1,5-bisphosphate carboxylase/oxygenase; SDS−PAGE, sodium dodecyl sulfate−polyacrylamide gel electrophoresis; Tween-20, polyoxyethylenesorbitan monolaurate; Tris, tris(hydroxymethyl)aminomethane.

0006-2960/95/0434-14932$09.00/0

energy for the release of unfolded proteins in a form that could partition to the native state. Central to this mechanism was the involvement of both toroids of GroEL in the protein folding reaction.

However, several members of the GroEL family have been purified as 7-mers, singly toroidal proteins, notably those from mammalian mitochondria (Viitanen et al., 1992), moth testis mitochondria (Miller et al., 1990) and *Thermoanaerobacter brockii* (Truscott et al., 1994). These single ringed GroELs represent an anomaly since current models for the function of the chaperonins [e.g., Todd et al. (1994)] consider the double-ringed structure as the minimal unit capable of facilitating protein folding under nonpermissive conditions. It therefore became imperative to determine if the single-ringed GroEL became a double-ringed structure, however transiently, under conditions of facilitated protein folding. Here we report the analysis of the *T. brockii* GroEL homologue (*Tbr*-EL). We demonstrate that this singly-toroidal chaperonin dimerizes in the presence of co-chaperonin, $GroES_7$, and Mg·ATP. Characterization of both the single- and the double-ring homologues revealed that double-ringed structures can have two peptide binding sites, one of which is blocked upon $GroES_7$ binding.

EXPERIMENTAL PROCEDURES

Proteins. *T. brockii* thermophilic chaperonins were purified as described previously (Truscott et al., 1994) and stored as an $(NH_4)_2SO_4$ precipitate. No change in distribution between 7-mer and 14-mer was observed upon storage. The precipitate was dissolved and desalted into 20 mM Tris-HCl, pH 7.7, 5 mM $MgCl_2$, 1 mM KCl, and 100 mM NaCl, prior to high-resolution gel-filtration chromatography (Bio-Sil SEC 400-5, 7.8 × 300 mm, or TSK 4000, 21.7 × 300 mm, typically run at 37 °C) using the buffers indicated in the figure legends. Only with ADP in the column buffer could *Tbr*-EL_7 and *Tbr*-EL_{14} be separated. No difference in the elution position was observed varying the concentration of ADP from 100 to 500 μM ADP, but because of the higher detection sensitivity at lower nucleotide concentration, 100 μM ADP was used in most experiments. Fractions of the two species of *Tbr*-EL were pooled, desalted to remove the residual ADP, and stored at 25 °C.

Escherichia coli chaperonin proteins were purified as described (Todd et al., 1993). Metabolic ^{35}S labeling of *E. coli* GroES and *Rhodospirillum rubrum* Rubisco and purification of isotopically pure proteins were as previously described (Todd et al., 1994). Concentrations of purified, labeled proteins were determined by activity.

Assays. ATPase assays were based upon molybdophosphate extraction of $^{32}P_i$ hydrolyzed from [γ-^{32}P]ATP as previously described (Todd et al., 1993). Rubisco folding assays were begun by adding acid-denatured Rubisco to GroEL at 10 °C in the absence of Mg^{2+}, which can increase the rate of Rubisco aggregation (M. J. Todd, unpublished results). During the short time (≤5 min) needed to efficiently bind the Rubisco at 10 °C, no significant cold-induced denaturation of *Tbr*-EL_{14}·*Tbr*-ES_7 occurred. The *Tbr*-EL·Rubisco complex was subsequently equilibrated at 37 °C, folding was initiated by the addition of ATP, and reactions were quenched with glucose/hexokinase (Todd et al., 1994). Rubisco activity was determined at 25 °C as previously decribed (Todd et al., 1994).

Analytical Gel Filtration Chromatography. Complexes of *Tbr*-EL were analyzed using high-resolution gel filtration chromatography (7.8 × 300 mm, 1 mL/min) equilibrated in either buffer A (20 mM Tris-HCl, pH 7.7, 5 mM $MgCl_2$, 50 mM KCl, 100 mM NaCl, 100 μM ADP) or buffer B (20 mM Tris-HCl, pH 7.7, 30 mM $MgCl_2$, 50 mM KCl, 100 μM ADP), as indicated. Columns were monitored using a Hewlet-Packard 1050 HPLC with diode array detection. Ligand binding was monitored either spectrophotometrically or radiometrically.

Ligand Binding. [^{32}P]Nucleotide binding was qualitatively analyzed using Bio-Sil SEC 400-5 and quantitated using P-10 resin (100−200 mesh, 10 × 80 mm) since incomplete recovery of GroEL is observed using TSK resin. Titrations (110 μL) contained 1.4 μM *Tbr*-EL_7 or 1.4 μM *Tbr*-EL_{14}·*Tbr*-ES_7 plus 200 μM ATP {[α-^{32}P]ATP (200 Ci/mol) or [γ-^{32}P]-ATP (100 Ci/mol)} and, where indicated, 2.1 μM *Eco*-ES_7 in buffer A to allow observation of both *Tbr*-EL species.

Quantitation of co-chaperonin binding was done by mixing 0.70 μM *Tbr*-EL_7 or 0.35 μM *Tbr*-EL_{14}·*Tbr*-ES_7 with 2 mM of the indicated nucleotide and 1.4 μM [^{35}S]*Eco*-ES_7 (27 Ci/mol) for 5 min and then analyzing by gel filtration. All reactions and chromatography were performed at 37 °C unless otherwise indicated.

Substoichiometric binding of unfolded [^{35}S]Rubisco was determined by challenging a mixture of 420 nM *Tbr*-EL_7 plus either 210 nM *Tbr*-EL_{14}·*Tbr*-ES_7 or 200 nM *Eco* -EL_{14} with 200 nM acid-denatured (van der Vies et al., 1992) [^{35}S] Rubisco (~900 Ci/mol). Loading of unfolded Rubisco onto GroEL species was done at 10 °C to minimize Rubisco aggregation, which would reduce the yield of bound proteins. Binding of saturating amounts of unfolded Rubisco was determined by challenging a mixture of 150 nM *Tbr*-EL_7 plus either 75 nM *Tbr*-EL_{14}·*Tbr*-ES_7 or 75 nM *Eco* -EL_{14}, with 600 nM acid-denatured [^{35}S]Rubisco (137 Ci/mol) (Figure 6). The resulting Rubisco−chaperonin complexes were rapidly warmed to 25 °C and analyzed by gel-filtration chromatography (TSK4000), also at 25 °C. Bound protein was quantitated by scintillation counting. All reactions and the column were equilibrated with buffer A.

Quantitation of unfolded Rubisco binding to various *Eco*-EL ± *Eco*-ES complexes was determined as above, using 150 nM *Eco*-EL_{14} ± 480 nM *Eco*-ES_7 in 20 mM Tris-HCl, pH 7.5, 5 mM $MgCl_2$, 0.5 mM KCl, and 0.5 mM EDTA. Since slight losses of GroEL occur using TSK resins, the mass of GroEL eluting from the column was determined spectrophotometrically at 225 nm. ATP (100 μM) was added prior to denatured Rubisco binding to quantitate Rubisco binding to the asymmetric complex. ATP added afterward allowed quantitation of the number of Rubisco released in forming the asymmetric chaperonin complex from *Eco*-EL with all binding sites for unfolded protein occupied by Rubisco. The low potassium and ATP concentrations prevented protein folding from occurring, thus allowing an observation of only the binding reaction.

RESULTS

T. brockii GroEL Oligomeric Structure

Analysis of purified Tbr-GroEL Reveals Two Species, Tbr-EL_7 and Tbr-EL_{14}·Tbr-ES_7. Purified GroEL preparations

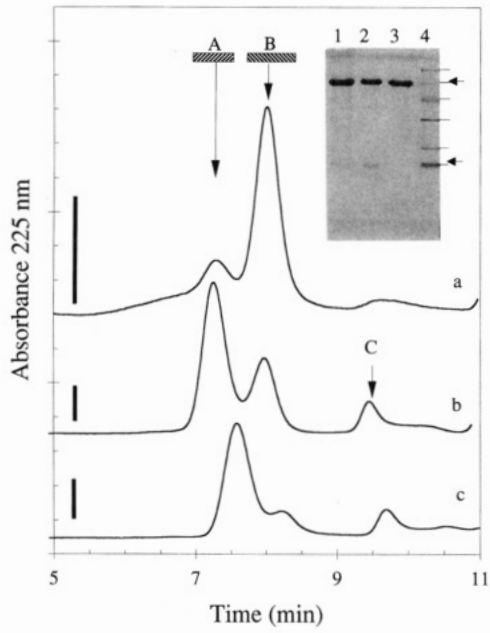

FIGURE 1: Purified GroEL from *T. brockii* analyzed by gel filtration chromatography. *T. brockii* (trace a: 88 pmol of protomer; Truscott et al., 1994) was analyzed on a TSK4000 (Bio-Rad) equilibrated with 20 mM Tris-HCl, pH 7.7, 5 mM $MgCl_2$, 50 mM KCl, 100 mM NaCl, and 100 μM ADP (buffer A), at 1 mL/min at 37 °C. Vertical bars indicate an optical density of 0.01 from an HP1050 DAD detector. Mammalian mitochondria GroEL$_7$ (*mt*-EL$_7$; Viitanen et al., 1992) and *Eco*-EL$_{14}$ (Todd et al., 1993) were used to standardize the column (arrows at 7.25 and 8.0 min, respectively). *Tbr*-EL$_{14}$ and *Tbr*-EL$_7$ were pooled separately (bars A and B, respectively). *Tbr*-EL conformers were reanalyzed, confirming ≥85% enrichment for *Tbr*-EL$_{14}$·*Tbr*-ES$_7$, and ≥95% enrichment for *Tbr*-EL$_7$. Dimerization of *Tbr*-EL$_7$ is Mg^{2+} dependent. *Tbr*-EL$_7$ (27 pmol) + 250 nmol of ATP + 180 pmol of *Eco*-ES$_7$ were incubated at 37 °C for 5 min and then analyzed by gel filtration (trace b, excess *Eco*-ES is identified by arrow c). Trace c is an identical reaction with incubation and analysis in buffer B (20 mM Tris-HCl, pH 7.7, 30 mM $MgCl_2$, 50 mM KCl, 100 μM ADP). All peaks (including *Eco*-EL$_{14}$ and mt-EL$_7$) elute ~0.5 min later in trace c due to effects on the chromatographic matrix. All injections were 100 μL. (*Inset*) SDS−PAGE on 3 μg each of (1) purified *Tbr* -EL applied to TSK 4000, (2) pool A from trace a, (3) pool B from trace a. Molecular weight standards (Bio-Rad, lane 4, shown top to bottom are as follows: phosphorylase B, 97.4 kDa; bovine serum albumin, 66.2 kDa; ovalbumin, 45 kDa; carbonic anhydrase, 31 kDa, soybean trypsin inhibitor, 21 kDa, and lysozyme, 14.4 kDa) are shown on the right and the positions of *Tbr*-EL and *Tbr*-ES are indicated with arrows. Buffer system was that of Lammeli, using a 15% resolving gel (84 × 50 × 0.75 mm), run at 10 W constant power and stained using Comassie blue.

from *T. brockii* were thought to consist predominantly of single-ringed structures (Truscott et al., 1994). Gel-filtration chromatography and gradient native-gel electrophoresis were previously used to identify species with molecular masses of ~400 and ~60 kDa, corresponding to heptameric and monomeric species, respectively (Truscott et al., 1994). This was unusual, since the GroEL homologue from *T. thermophilus* not only purified as a tetradecamer of 60 kDa subunits but also contained stably bound *Tth*-ES and ADP (Taguchi et al., 1991).

High-resolution gel-filtration chromatography of *Tbr*-EL preparations [using *Eco*-EL$_{14}$ and mammalian mitochondrial GroEL (*mt*-EL$_7$) as standards] revealed a mixture of tetradecameric and heptameric species (Figure 1, trace a). In column buffers lacking nucleotide these two species migrated with an intermediate molecular weight and could not be resolved (S. Walke, unpublished results). Fractions containing 14-mer and 7-mer were pooled and desalted (Figure 1, trace a, bars A and B). Both species had subunits with 60 kDa molecular mass and appeared ≥95% pure by SDS−PAGE (Figure 1, inset). The fraction eluting as a 14-mer (bar A of Figure 1, trace a) also contained a minor band at ~14 kDa (Figure 1, inset). N-terminal sequence analysis of the 14 kDa band (data not shown) gave a sequence 100% identical to that reported previously for *Tbr*-ES (Truscott et al., 1994). Sequence analysis of the 60 kDa bands (16 residues) in lanes 2 and 3 demonstrated complete homology to *Tbr*-EL. The two pools were therefore referred to as *Tbr*-EL$_7$ and *Tbr*-EL$_{14}$·*Tbr*-ES$_7$.

Table 1: *Tbr*-EL$_7$ Dimerization: Ligand Requirements

condition[a]	% *Tbr*-EL$_{14}$	
	5 mM Mg^{2+}	30 mM Mg^{2+}
1 *Tbr*-EL$_7$	0%	0%
2 *Tbr*-EL$_7$ + ATP	0%	0%
3 *Tbr*-EL$_7$ + *Eco*-ES	0%	10%[b]
4 *Tbr*-EL$_7$ + ATP + *Eco*-ES	70%	95%
5 *Tbr*-EL$_7$ + ADP + *Eco*-ES	0%	30%
6 *Tbr*-EL$_7$ + γ-S-ATP + *Eco*-ES	37%	nd[c]
7 *Tbr*-EL$_7$ + AMP-PNP + *Eco*-ES	78%	82%
8 *Tbr*-EL$_7$ + Ru-A ± *Eco*-ES	0%	nd

[a] Incubations contained 200 nM *Tbr*-EL$_7$, plus the following, when indicated: 600 nM *Eco*-ES$_7$, 2 mM nucleotide, or 600 nM acid-denatured Rubisco, in buffer A (minus ADP, first column) or buffer B (minus ADP, second column). Reactions were then analyzed by gel filtration in buffer A (first column) or buffer B (second column) after 5 min incubation. All reactions and analyses were at 37 °C. [b] In the absence of ADP in the column elution buffer, no distinction between heptameric and tetradecameric species was possible. This sample, incubated in the absence of nucleotide, may have assembled following injection onto the column equilibrated with ADP before separation of *Eco*-ES$_7$ and heptameric *Tbr*-EL$_7$ species. [c] nd, not determined.

Upon further analysis of either purified Tbr-EL species, a single peak was obtained, demonstrating ≥95% enrichment for *Tbr*-EL$_7$ and ≥90% enrichment for *Tbr*-EL$_{14}$·*Tbr*-ES$_7$ (data not shown). The stability of these two species following buffer exchange suggested that the spontaneous interconversion was slow, regardless of the presence of nucleotide. Thus the heptamer and tetradecamer were not in rapid equilibrium, but distinct, stable species. The residual heptamer in the tetradecamer preparation (~8%) was not a product of 14-mer dissociation, since this fraction did not increase with time (~10% heptamers seen after 6 weeks at 25 °C). In the absence of Mg^{2+}, or at low temperatures (0 °C), spontaneous dissociation of both species to monomers was more rapid, as previously observed (Truscott et al., 1994; see below).

Dimerization of Tbr-EL$_7$ Species. Dimerization of heptameric species was studied using various ligands typically included in the protein folding reaction. The conditions for converting *Tbr*-EL$_7$ to the asymmetric *Tbr*-EL$_{14}$·*Eco*-ES$_7$ complex are listed in Table 1. In the presence of ATP and *Eco*-ES$_7$, but neither ligand alone, ~70% of heptamer could dimerize (Figure 1, trace b; Table 1, entries 1−4). Increasing the Mg^{2+} concentration increased the yield of tetradecamer even further, to 80−90% (Figure 1, trace c; Table 1, entry 4). The GroES$_7$ requirement was absolute and stoichiometric; substoichiometric amounts of *Eco*-ES$_7$ only allowed formation of one molar equivalent (with respect to *Eco*-ES$_7$) of *Tbr*-EL$_{14}$·*Eco*-ES$_7$ (M. J. Todd, unpublished results). We have been unable to demonstrate the existence of stable *Tbr*-EL$_{14}$ when GroES is rigorously excluded, suggesting that

stable formation of the thermophilic 14-mer may depend upon the binding of GroES. In this respect it would resemble the GroEL of *T. thermophilus* which is purified as a stable complex together with GroES (Taguchi et al., 1991). Chaperonin complex could form using ADP (Table 1, entries 3 and 5); however, net assembly of tetradecamer was poor and only occurred at elevated concentrations of Mg^{2+}. The incomplete assembly of *Tbr*-EL_7 at lower Mg^{2+} concentrations was surprising since, once formed, isolated *Tbr*-EL_{14}·ES_7 was stable (see below). When *Tbr*-EL_7 which failed to assemble was purified and again used in the dimerization reaction, repartitioning between *Tbr*-EL_7 and *Tbr*-EL_{14}·ES_7 occurred. The reason for this apparent paradox is unclear but is consistent with an additional role for Mg^{2+} in chaperonin function other than simply nucleotide chelation. Additional roles for Mg^{2+} on *E. coli* chaperonin structure (Azem et al., 1994a) and complex stability (Azem et al., 1994b; Todd et al., 1994) have previously been proposed. Nucleotide analogs supported heptamer dimerization (Table 1, entries 6 and 7), suggesting that binding of a triphosphonucleotide was sufficient for assembly; hydrolysis was not required.

Unfolded proteins bound to *Eco*-EL_{14} markedly stabilized the chaperone from urea induced denaturation and promoted tetradecamer formation from monomers (Mendoza et al., 1994), presumably due to multivalent binding of unfolded proteins to individual chaperonin subunits. Accordingly, we analyzed whether unfolded proteins could induce dimerization of *Tbr*-EL_7. Table 1, entry 8, reveals that unfolded Rubisco did not induce dimerization, suggesting that polypeptide binding to a single $GroEL_7$ toroid sterically precludes simultaneous stable binding of the same peptide to a second toroid.

The effect of temperature, protein concentration, and time on the formation of *T. brockii* GroEL tetradecamers was systematically analyzed in order to better understand the assembly reaction. Heptamer dimerization in 5 mM Mg^{2+} (where dimerization did not proceed to completion) was optimal at 35−45 °C (Figure 2A). Neither higher temperatures during the assembly reaction nor elevating the column temperature (to 50 °C) increased the amount of tetradecamer. We cannot, however, exclude the possibility that the *Eco*-ES_7 became unstable at elevated temperatures thus decreasing the recovery of tetradecamer. Control experiments determining *Eco*-ES_7 thermostability showed that after 30 min at 80 °C *Eco*-ES_7 could still support protein folding at 25 °C (M. J. Todd, unpublished results). However, renaturation of a thermally denatured species upon lowering the temperature has not been ruled out.

The extent of *Tbr*-EL_7 dimerization was dependent upon both heptamer and Mg^{2+} concentrations (Figure 2B). At 30 mM Mg^{2+}, the maximum yield of tetradecamer (80−90%, Figure 1, trace c; Table 1, entry 4) was obtained at *Tbr*-EL_7 concentrations in excess of 0.1 μM (protomer). At 5 mM Mg^{2+} ~5-fold higher concentrations of *Tbr*-EL_7 were required for maximum dimerization. Consistent with the above results, a decrease in the yield of *Tbr*-EL_{14}·*Eco*-ES_7 formed was observed at reduced Mg^{2+} concentrations.

Since *Tbr*-EL_7 hydrolyzes ATP at ~2 min^{-1}, we expected that optimal dimerization should require at least 30 s. The dimerization reached 80−90% following multiple turnovers, yet ≤10% formed starting from ADP (Table 1, entries 3 and 5). A time course for complex formation at 1.0 μM *Tbr*-EL

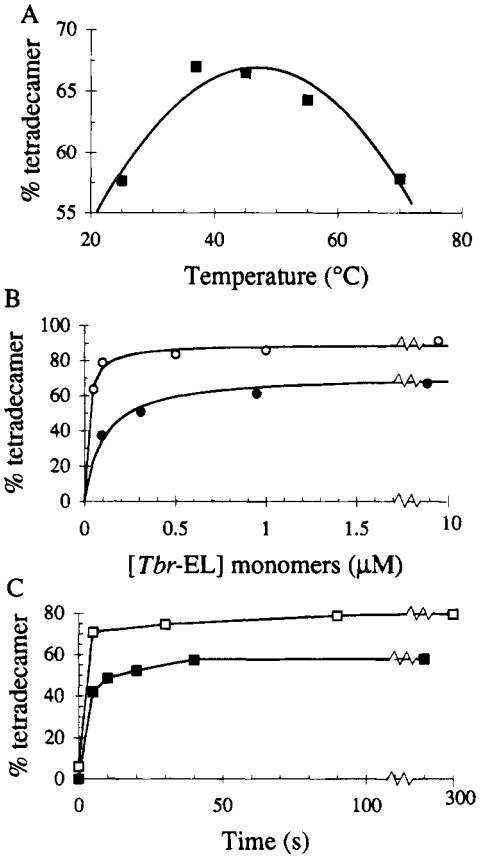

FIGURE 2: (A) Percent *Tbr*-EL_{14} (relative to total mass eluting) as a function of temperature. *Tbr*-EL_7 (27 pmol) was incubated 5 min with 180 pmol of *Eco*-ES_7 and 230 nmol of ATP at 37 °C and then analyzed by gel filtration in buffer A. (B) Dimerization of *Tbr*-EL_7 as a function of concentration in buffer A (●) or buffer B (○). Incubation was as in panel A, using constant 250 pmol of *Eco*-ES_7. (C) Dimerization of 28 pmol of *Tbr*-EL_7 as a function of time in buffer A (●) or buffer B (○). Incubation was as in panel A and included 60 pmol of *Eco*-ES_7 and 23 nmol of ATP. Reactions were quenched at the indicated times with glucose/hexokinase (40 mM glucose, 27 units/mL hexokinase). Addition of the quench 3 ± 1 s prior to addition of *Tbr*-EL_7 prevented assembly (see Table 2). One hundred microliters of each 110 μL reaction was analyzed by gel filtration chromatography.

protomer in 5 mM and 30 mM Mg^{2+}/0.2 mM ATP is shown in Figure 2C. *Tbr*-EL_7 became committed to dimerize with a half-time of <5 s even though 30 s was required for complete turnover. These results were consistent with our ability to form tetradecamer using nonhydrolyzable analogs (Table 1, entry 8) and indicated that, upon ATP binding, the commitment to dimerization is rapid. The absolute requirement for a GroES homologue (Table 1) and the inability to isolate a stably bound GroES in the absence of nucleotide (data not shown) suggested that GroES interacts rapidly with ATP bound *Tbr*-EL_7 and that prior to hydrolysis this complex became committed to dimerize.

The committed species observed in Figure 2C are actually the sum of *Tbr*-EL_7 dimers (i.e., double rings) already existing at the time of the quench plus those *Tbr*-EL_7 (single rings) which are committed to becoming double rings (perhaps by virtue of having already sequestered ATP and $GroES_7$). The following pulse−chase experiment was designed to determine the fraction which already existed as double rings at the time of the quench. Ten picomoles of *Tbr*-EL_7 was incubated with 30 pmol of *Eco*-ES_7 and ATP for 3 s, and then a glucose/hexokinase quench was introduced

Table 2: Rapid Dimerization of *Tbr*-EL_7·ATP_7·*Eco*-ES_7

experiment	additions[a] at 0 s	additions[a] at 3 s	additions[a] at 6 s	pmol isolated as 14-mer	pmol isolated as 7-mer
quench added first: <5% dimerize	quench	ATP		0.4	9.7
after 3 s, >80% are committed to dimerize	ATP	quench		8.2	1.8
committed complexes cannot recuit additional toroids	ATP	quench	*Tbr*-EL_7	10.4	9.7

[a] All reactions contained 10 pmol of *Tbr*-EL_7 and 300 pmol of *Eco*-ES_7 in 100 μL of buffer B. Additions include the following: quench (glucose to 10 mM, 4.3 units of hexokinase); ATP (to 2 mM); and *Tbr*-EL_7 (10 additional pmol). Reactions (at 25 °C) were allowed to come to equilibrium and then were analyzed by gel-filtration chromatography in buffer B.

Table 3: Stability of Asymmetric Complex Depends on GroES

condition[a]	time (min)	ES homolog: *Eco*-ES_7 % 14-mer	ES homolog: *Tbr*-ES_7 % 14-mer
control	120	85%[b]	90%
0 °C	90	13%	83%
+50 mM EDTA	20	60%	84%

[a] 2.2 μM *Tbr*-EL_7 was incubated with excess $GroES_7$ and 0.5 mM ATP in buffer B for 5 min and then isolated by gel-filtration into buffer B (see Figure 1, trace c). Asymmetric complex was concentrated and then diluted 50-fold with buffer B minus ADP to reduce the nucleotide concentration. ADP external to the asymmetric complex is known to inhibit spontaneous dissociation (Todd et al., 1994). Stability is expressed as remaining tetradecameric species following the given treatment. Both control and EDTA reactions were at 25 °C. [b] Values are accurate to within ±5%.

to hydrolyze the remaining available ATP. During this time, 80−90% of *Tbr*-EL_7 became committed to forming tetradecamer (Figure 2C and Table 2), yet only ~10% of the molecules had hydrolyzed the ATP *(see ATPase Activity of Tbr-EL_7 and Tbr-EL_{14}·Tbr-ES_7)*. We demonstrated above the rapid formation of a ternary complex, *Tbr*-EL_7·ATP_7·*Eco*-ES_7, which is committed to dimerize. If this species existed entirely as dimers (after 3 s), additional *Tbr*-EL_7 would not be recruited into 14-mer. On the other hand, if rapid formation of *Tbr*-EL_7·ATP_7·*Eco*-ES_7 was followed by slow recruitment of *Tbr*-EL_7 (±ANP), much of the additional *Tbr*-EL_7 (the 10 pmol introduced at 6 s) should be recruited into 14-mers. Our results (Table 2, line 3), suggest that most of the *Tbr*-EL_7·ATP_7·*Eco*-ES_7 had already dimerized within 3s, thus minimizing the recruitment of additional *Tbr*-EL_7 following the quench.

Dissociation of Tbr-EL_{14}·Tbr-ES_7 Complexes. Tetradecameric *Tbr*-EL_{14}·ES_7 was relatively stable at 25 °C in the presence of Mg^{2+}. Simulation of folding conditions (addition of GroES, K^+, Mg^{2+}, and ATP) did not cause measurable dissociation of tetradecamer, suggesting that dissociation to the 7-mer occurred during purification and was not an intrinsic part of the chaperonin reaction cycle. Slow dissociation of the doubly toroidal species could be induced by lowering the temperature or through Mg^{2+} chelation using EDTA (Table 3). The heterologous tetradecamer (*Tbr*-EL_{14}·*Eco*-ES_7) was significantly less stable than the homologous tetradecamer (*Tbr*-EL_{14}·*Tbr*-ES_7), dissociating >10-fold faster at 0 °C or >3-fold faster upon addition of EDTA. When formed using [^{35}S]*Eco*-ES_7, dissociation of the *Tbr*-EL_{14}·*Eco*-ES_7 complex (as measured by change in molecular weight on gel-filtration columns) parallelled loss of [^{35}S]*Eco*-ES_7 (M.J.T., unpublished observations). Thus, the persistence of the *T. brockii* GroEL tetradecamer depended upon the binding of a $GroES_7$ homologue. No appearance of monomeric species was detected under protein folding conditions (5 mM Mg^{2+}, K^+, ATP, with or without GroES), suggesting that dissociation to monomers is not part of the normal *Tbr*-GroEL chaperonin protein folding cycle. GroEL homologues from *E. coli* (Goloubinoff et al., 1989), *T. thermophilus* (Taguchi et al., 1991), and chloroplasts (Musgrove et al., 1987) were demonstrated to form faster-migrating species on native gels following turnover, consistent with ATP-induced dissociation into smaller species. However, the native-gel chromatography subjects the proteins to nonequilibrium conditions that may induce a small portion of the complexes to dissociate.

ATPase Activity of Tbr-EL_7 and Tbr-EL_{14}·Tbr-ES_7

Our initial attempts to fold proteins using *T. brockii* GroEL showed a loss of activity after desalting and led to the discovery that this chaperonin only functions at elevated concentrations of monovalent cations. *E. coli* GroEL will fold *R. rubrum* Rubisco at its maximum rate in 1 mM ATP and 1 mM K^+ (Viitanen et al., 1990). Both *Tbr*-EL_7 and *Tbr*-EL_{14}·*Tbr*-ES_7, however, were inactive using these same conditions. We therefore began a systematic examination of *T. brockii* ATP hydrolysis and protein folding activities.

ATP hydrolysis by *Tbr*-EL_7 and *Tbr*-EL_{14}·*Tbr*-ES_7 was first examined as a function of monovalent cation. Slow ATP hydrolysis was observed even in the absence of added K^+; thus, unlike *Eco*-EL_{14}, the K^+ requirement was not absolute. *Tbr*-EL_7 ATPase activity increased ~5-fold upon K^+ addition (Figure 3A). A half-maximal rate of ATP hydrolysis (100 μM ATP) was observed at 13 ± 3 mM K^+ with *Tbr*-EL_7, and at 9 ± 2 mM K^+ with *Tbr*-EL_{14}·*Tbr*-ES_7. K^+ activation followed simple binding; no cooperativity was detected. This ion requirement was 1000-fold greater than that seen for *Eco*-EL_{14} (Todd et al., 1993), where ~10 μM K^+ was required for half-maximal activation of the ATPase (also measured with 100 μM ATP). The ATPase was specific for NH_4^+ or K^+; Na^+ could not substitute. Thus further characterization was carried out at 50 mM K^+. The maximum ATPase activity of *Tbr*-EL_7 agreed well with that reported previously [2.4 min^{-1} (Truscott et al., 1994)]. Note that, under these conditions (no GroES present), *Tbr*-EL_7 could not dimerize to form stable tetradecameric structures.

The co-chaperonin GroES is essential under conditions where a substrate protein cannot spontaneously fold (Schmidt et al., 1994a). *Eco*-ES_7 binds at one end of *Eco*-EL_{14}, forming an asymmetric bullet-shaped structure (Saibil et al., 1991; Langer et al., 1992; Azem et al., 1994b; Schmidt et al., 1994b). Formation of this complex with the homologous *E. coli* system results in either 50% or 100% inhibition of the GroEL ATPase, depending upon the K^+ concentration (Viitanen et al., 1990; Gray & Fersht, 1991; Todd et al., 1993). This complex, however, only forms after one toroid of GroEL has hydrolyzed ATP at an uninhibited rate; thus

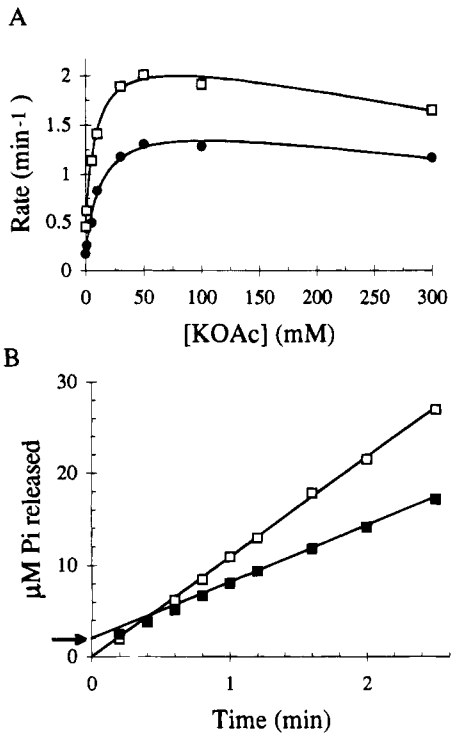

FIGURE 3: (A) Initial rates of ATP hydrolysis by *Tbr*-EL_7 (□) and *Tbr*-EL_{14}·*Tbr*-ES_7 (●) as a function of potassium concentration. $^{32}P_i$ release was measured in 50 mM Tris-HCl, pH 7.8, 0.5 mM EDTA, and 10 mM $MgCl_2$ (buffer C) with 72 nM *Tbr*-EL_7 or 18 nM *Tbr*-EL_{14}·*Tbr*-ES_7 plus various amounts of KOAc. Linear regression analysis of ≥4 time points ($r \geq 0.995$ with <10% substrate hydrolyzed) gave initial rates. (B) Initial rate of ATP hydrolysis by 0.71 μM *Tbr*-EL_7 plus 0 (□) or 1.44 (■) μM *Eco*-ES_7 in buffer C plus 50 mM KCl. All ATP hydrolysis assays were done at 37 °C with 200 μM [γ-^{32}P]ATP as described (Todd et al., 1993).

in the presence of GroES a pre-steady-state burst in $^{32}P_i$ release is observed (Todd et al., 1993). Subsequent turnovers were proposed to be at the same rate, by only one-half of the sites, thus the 50% decrease in the rate of ATP hydrolysis (Todd et al., 1993).

We performed a similar analysis of heptameric and tetradecameric *Tbr*-EL ATPase, searching for both GroES inhibition and pre-steady-state bursts. The rate of ATP hydrolysis by *Tbr*-EL_7 alone was ~2 min^{-1}. As with *Eco*-EL_{14} (Todd et al., 1993), *Tbr*-EL_7 displayed no pre-steady-state burst of product formation in the absence of GroES. However, in the presence of *Eco*-ES_7, the steady-state rate of ATP hydrolysis by *Tbr*-EL_7 was 50% decreased to 1 min^{-1} and followed a pre-steady-state burst of 0.4 mol of ATP hydrolyzed per mol of protomer (Figure 3B), similar to that observed with the *E. coli* chaperonins (Todd et al., 1993). In contrast, the rate of ATP hydrolysis by *Tbr*-EL_{14}·*Tbr*-ES_7 was initially 50% that of *Tbr*-EL_7 (1 min^{-1}), and, upon addition of *Eco*-ES_7, no change in rate was observed (data not shown). This result was expected, since the high molecular weight *T. brockii* GroEL already contained a stoichiometric amount of *Tbr*-ES_7. Inhibition of either species by *Eco*-ES_7 was not dependent on the concentration of monovalent cation.

Stable Ligand Binding by Tbr-EL$_7$ and Tbr-EL$_{14}$·Tbr-ES$_7$

[^{32}P]ADP Binding. *Eco*-EL_{14} forms a stable, isolatable complex with 1 mol of *Eco*-ES_7 and 7 mol of ADP per mol of complex (Todd et al., 1993). The *T. thermophilus* GroEL copurified as a complex with ADP and GroES, demonstrating the tight binding of the co-chaperonin (Taguchi et al., 1991). Since *Tbr*-EL_7 dimerization required both nucleotide and *Eco*-ES_7, it was probable that the stability of the tetradecameric complex was maintained through tight binding of these ligands.

Table 4: Quantitation of Ligand Binding

condition	starting species: *Tbr*-EL_7[a] (mol / mol 14-mer)	starting species: *Tbr*-EL_{14}·*Tbr*-ES_7[a] (mol / mol 14-mer)
1 [γ-^{32}P]ATP ± *Eco*-ES	≤0.1	≤0.06
2 [α-^{32}P]ATP	nd[b]	5.2[c]
3 [α-^{32}P]ATP + *Eco*-ES	6.0[c]	4.6[c]
4 [α-^{32}P]ATP + *Tbr*-ES	6.4[c]	5.3[c]
5 [^{35}S]*Eco*-ES + ATP	0.97	0.46
6 [^{35}S]*Eco*-ES + AMP-PNP	1.05	nd[b]

[a] Refers to the chaperonin species initially present in the reaction. [^{32}P]Nucleotide and [^{35}S]GroES counts were only found associated with 14-mer peak (Figure 4). See Experimental Procedures for concentration of proteins and nucleotides. [b] nd, not determined. [c] Quantitation of [α-^{32}P]ADP was performed on P-10 resin due to interference from the TSK 4000 matrix.

Tbr-EL_7 was incubated with [^{32}P]nucleotide and isolated from free nucleotide by gel filtration (in the presence of unlabeled ADP) to determine stably bound nucleotide. Little nucleotide co-eluted with purified *Tbr*-EL_7 species in the absence of added $GroES_7$, because all bound nucleotide exchanged during gel-filtration chromatography (Table 4, entry 2). On the other hand, *Tbr*-EL_{14}·*Tbr*-ES_7 stably bound [α-^{32}P]ADP, even in the absence of added co-chaperonin (Table 4, entries 2 and 4). GroES binding was previously shown to be necessary to sequester tightly bound nucleotide on *Eco*-EL_{14} (Todd et al., 1993, 1994). The similar stoichiometry of nucleotide binding to *Tbr*-EL_{14}·*Tbr*-ES_7, independent of added GroES, was therefore consistent with *Tbr*-EL_{14}·*Tbr*-ES_7 already containing a stoichiometric amount of co-chaperonin. Upon addition of *Eco*-ES_7, *Tbr*-EL_7 could also bind [α-^{32}P]ATP (Figure 4; Table 4, entries 3 and 4), but not [γ-^{32}P]ATP (Table 4, entry 1), indicating that the ATP initially trapped in the complex had already undergone hydrolysis. Stably bound nucleotide was only associated with the tetradecamer peak, even under conditions where both species could be observed (Figure 4). Quantitation of tightly bound [α-^{32}P]ADP revealed >6 mol of ADP bound per mol of tetradecameric complex. At lower Mg^{2+} concentrations, lower site occupancy and a trailing edge to the [α-^{32}P]ADP co-eluting with tetradecamer was consistent with slow dissociation of the complex. Slightly greater amounts of bound nucleotide could be isolated when forming the complex using *Tbr*-ES_7 than with the *Eco*-ES_7, consistent with the greater stability of the homologous complex (compare Table 4, entries 3 and 4).

[^{35}S]Eco-ES$_7$ Binding. $GroES_7$ binding to *Tbr*-EL_7 and *Tbr*-EL_{14}·*Tbr*-ES_7 was examined using metabolically labeled [^{35}S]*Eco*-ES_7. Upon addition of nucleotide, stable binding of *Eco*-ES_7 only to tetradecameric *Tbr*-EL_{14} could be detected (Figure 4). Quantitation of bound [^{35}S]*Eco*-ES_7 demonstrated ~1 mol bound per mol of 14-mer when forming the complex starting with heptamer (Table 4, entry 5), less when using tetradecameric complex. The lower stoichiometry suggested

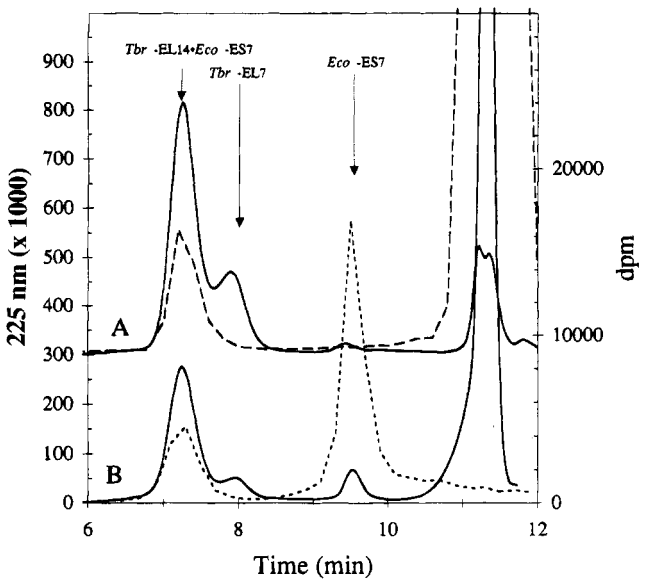

FIGURE 4: Ligands bind stably to tetradecamer. *Tbr*-EL_7 in buffer A was incubated 5 min with *Eco*-ES_7 and [α-^{32}P]ATP (A) and then analyzed by gel filtration chromatagrphy (see Experimental Procedures). Absorbance at 225 nm (solid line, displaced upwards by 300) and dpm (dotted line, displaced upward by 10 000 dpm) are shown. (B) *Tbr*-EL_7 in buffer B was incubated 5 min with ATP plus [^{35}S]*Eco*-ES_7 as described in Experimental Procedures.

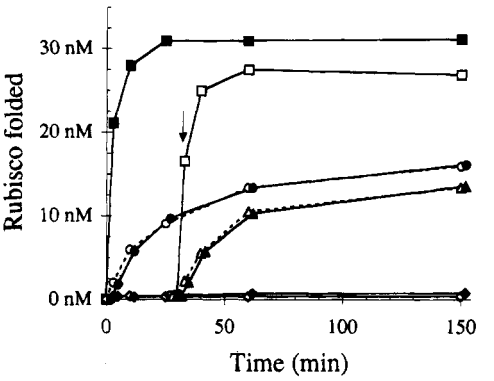

FIGURE 5: Rubisco folding activity with various chaperonins. Acid-denatured Rubisco (37 nM) was loaded onto 125 nM *Eco*-EL_{14} (■), 125 nM *Tbr*-EL_7 (○), or 125 nM *Tbr*-EL_{14}•*Tbr*-ES_7 (●) with 270 nM GroES present. At $T = 0$, ATP (to 1 mM) was added to initiate folding. In the absence of additional *Eco*-ES_7, neither *Tbr*EL_7 (◇) nor *Tbr*-EL_{14}•*Tbr*-ES_7 (◆) could support folding. Delayed addition of ATP to assays containing *Eco*-ES_7 plus *Eco*-EL_{14} (□), *Tbr*-EL_7 (△), or *Tbr*-EL_{14}•*Tbr*-ES_7 (▲) (arrow, chaperonin concentrations were as indicated previously), demonstrated that all species tested suppressed aggregation. Final concentrations of buffer components in the folding reaction were 100 mM HEPES, pH 7.8, 50 mM KOAc, 10 mM MgOAc, 10 mM DTT, 0.5 mM EDTA, and 0.01% Tween-20.

that *Tbr*-ES_7 (stably bound to purified *Tbr*-EL_{14}•*Tbr*-ES_7) diluted the specific activity of the *Eco*-ES_7. However, had the two GroES bound with the same affinity, we would have expected *Tbr*-EL_{14} to bind 80−90% as much *Eco*-ES_7 as *Tbr*-ES_7 when challenged with a 10-fold excess. Experimentally, only a 50% molar equivalence of [^{35}S]*Eco*-ES_7 was isolated as a complex with *Tbr*-EL_{14}, suggesting that *Tbr*-EL_{14} has a ~10-fold higher affinity for the homologous *Tbr*-ES_7. This result was consistent with the greater stability of the homologous asymmetric complex demonstrated in Table 3. On the basis of the above nucleotide binding titration, all of the *Tbr*-EL_{14}•*Tbr*-ES_7 had dissociated and re-formed using these conditions, so incomplete dissociation could not explain the lower stoichiometry of *Eco*-ES_7 binding.

Quantitative binding of *Eco*-ES_7 was also observed using AMP-PNP instead of ATP as the nucleotide when forming the complex (Table 4, entry 6). Little bound *Eco*-ES_7 could be detected when assembly was initiated with ADP. Thus, in the presence of a triphosphate nucleotide analog, *Eco*-ES_7 binding was stable enough to permit stoichiometric isolation of the asymmetric complex.

Interactions with Substrate Proteins

Protein Folding Activity. The ubiquitous presence of chaperonins is due to their ability to inhibit aggregation, release unfolded proteins, and assist in their proper folding. Activity of these three partial reactions was tested with both thermophyllic chaperonin species. Separately, *Tbr*-EL_7 and *Tbr*-EL_{14}•*Tbr*-ES_7 were incubated with acid denatured Rubisco, and the folding reaction (under nonpermissive conditions) was begun at 0 or 30 min by adding ATP (±*Eco*-ES_7). Figure 5 demonstrates that, in the absence of either nucleotide or *Eco*-ES_7, no folding was observed. Facilitated folding by both *Tbr*-EL_7 and *Tbr*-EL_{14}•*Tbr*-ES_7 required ATP and *Eco*-ES_7, despite the presence of a molar equivalent of *Tbr*-ES_7 already present in the latter species. Delayed addition of ATP (for up to 30 min) confirmed that the both species could suppress aggregation, implying the formation of a stable binary complex (unfolded protein−chaperonin). We note that the conditions necessary for nonpermissive folding to occur (the presence of MgATP and GroES) are also those which lead to the rapid conversion of the *Tbr*-EL_7 to the double-ringed complex. We conclude that although a single-ringed chapeornin is sufficient to supress aggregation, a doubly toroidal chaperonin is required to facilitate protein folding under nonpermissive conditions.

[^{35}S]Rubisco Binding. Chaperonins tightly bind unfolded proteins, thus preventing aggregation both in vivo and in vitro (Buchner et al., 1991). We used this tight binding to quantitate the amount of acid denatured [^{35}S]Rubisco bound to both heptameric and tetradecameric chaperonins by separating chaperonin-bound unfolded protein from aggregates. All chaperonin species efficiently and stably bound unfolded Rubisco.

The two *T. brockii* GroEL species could, however, have different affinities for unfolded proteins. Therefore, a mixture of *Tbr*-EL_7 and *Tbr*-EL_{14}•*Tbr*-ES_7 was challenged with substoichiometric amounts of unfolded Rubisco, and the partitioning of unfolded Rubisco to each species was quantitated. In a mixture of heptamers and tetradecamers of equal mass (twice as many heptameric particles), half as much [^{35}S] Rubisco bound per mol of heptamer (Table 5). This result suggested that *Tbr*-EL_7 had lower affinity than *Tbr*-EL_{14}•*Tbr*-ES_7 for unfolded protein. When the experiment was repeated using *Tbr*-EL_7 and *Eco*-EL_{14}, 4-fold more [^{35}S]Rubisco bound to *Eco*-EL_{14}, suggesting that the *E. coli* tetradecamer had either two binding sites (each with 2-fold higher affinity) or one binding site of 4-fold higher affinity than *Tbr*-EL_7.

The total number of binding sites was therefore quantitated using an excess of unfolded protein over the total concentration of toroids. Figure 6 and Table 5 reveal at most 1 mol of unfolded Rubisco bound to *Tbr*-EL_7, but significantly greater than 1 mol of Rubisco could be bound to *Eco*-EL_{14}.

Table 5: Quantitation of Acid-Denatured [^{35}S]Rubisco Binding

condition[a]	mol Rubisco / mol particle: *Tbr*-EL_7	*Tbr*-EL_{14}·*Tbr*-ES_7	*Eco*-EL_{14}
titration with subsaturating [^{35}S]Rubisco			
Tbr-EL_7 + *Tbr*-EL_{14}·*Tbr*-ES_7	0.21	0.42	
Tbr-EL_7 + *Eco*-EL_{14}	0.15		0.6
titration with saturating [^{35}S]Rubisco			
Tbr-EL_7 + *Tbr*-EL_{14}·*Tbr*-ES_7	0.77	0.79	
Tbr-EL_7 + *Eco*-EL_{14}	0.87		1.6
E. coli chaperonin controls			
Eco-EL_{14} + [^{35}S]Rubisco			1.75
Eco-EL_{14}·*Eco*-ES_7 + [^{35}S]Rubisco			0.95
Eco-EL_{14} + [^{35}S]Rubisco + *Eco*-ES/ADP			1.49

[a] See Figure 6 and Experimental Procedures for description of binding reactions.

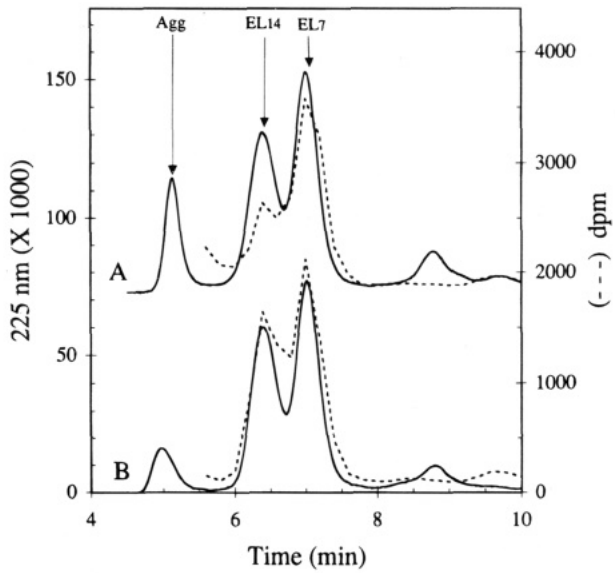

FIGURE 6: Titration of acid denatured [^{35}S]Rubisco binding. An equal mass of *Tbr*-EL_{14}·*Tbr*-ES_7 and *Tbr*-EL_7 (A) or an equal mass of *Eco*-EL_{14} and *Tbr*-EL_7 (B) was challenged with a 2−3-fold excess of acid-denatured Rubisco (see Experimental Procedures). Absorbance at 225 nm (solid lines) and dpm (dashed lines) (top data displaced upward by 0.075 and 1900 dpm, respectively) demonstrate twice as much Rubisco bound to doubly toroidal *Eco*-EL_{14} as bound to *Tbr*-EL_{14}·*Tbr*-ES_7 on a molar basis. Note that with an excess of Rubisco over GroEL binding sites, a large peak of aggregates elutes at 5 min.

The incomplete site occupancy of [^{35}S]Rubisco on all chaperonin species may be due to the presence of low-abundance, advantitiously bound, contaminating proteins which co-purify with chaperonin preparations (Hayer-Hartl & Hartl, 1993). Therefore, we conclude that upon complete saturation both the singly toroidal *Tbr*-EL_7 and the doubly toroidal *Eco*-EL_{14} can bind one unfolded protein per toroid.

Similar measurements of the stoichiometry of [^{35}S]Rubisco binding to the preformed asymmetric complexes *Tbr*-EL_{14}·*Tbr*-ES_7 and *Eco*-EL_{14}·*Eco*-ES_7 were made (Table 5). An approximately equal mass of *Tbr*-EL_7 was included as an internal standard (as in Figure 6, trace a). In both cases the asymmetric complexes could only bind half as much unfolded Rubisco as the *Tbr*-EL_7 internal standard (Table 5). Therefore, GroES binding inhibits one of the two GroEL toroids from binding unfolded protein tightly, leaving only one toroid free to interact with unfolded proteins.

Scheme 1

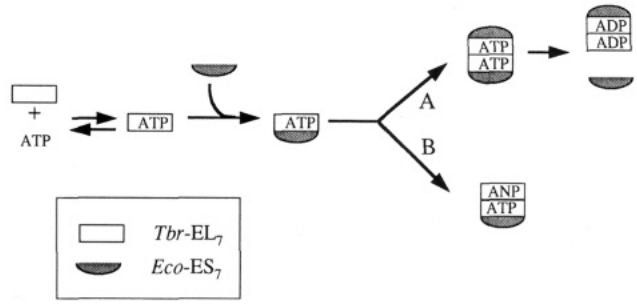

Next we inquired if binding of GroES displaced one of the two protein ligands. Starting with an *Eco*-EL_{14} with two molecules of unfolded [^{35}S]Rubisco bound (presumably one at either end), GroES and ADP were added to form the asymmetric complex. The results of this experiment (Table 5) revealed that little of the tightly bound protein was released upon formation of the asymmetric complex; i.e., significantly greater than 1 mol of unfolded protein per mol of complex remained bound. The asymmetric complex, formed in this manner, must therefore contain one unfolded protein on the *same* GroEL toroid as $GroES_7$ [consistent with previous cross-linking experiments (Bochkareva & Girshovich, 1992)] and a second on the opposing GroEL toroid.

DISCUSSION

Preparations of *Tbr*-EL have been resolved into two stable fractions according to size: (1) an oligomer of approximate molecular mass 400 kDa, containing only 60 kDa *Tbr*-EL subunits, which we identify as a single heptameric ring, *Tbr*-EL_7, and (2) an oligomer of approximate molecular mass 800 kDa, containing both 60 kDa *Tbr*-EL subunits and 10 kDa *Tbr*-ES subunits, which we identify as *Tbr*-EL_{14}·ADP_7·*Tbr*-ES_7. *Tbr*-EL_7 was rapidly ($t_{1/2}$ < 3 s) converted to the larger complex upon the addition of *Eco*-ES_7 and MgATP, with the incorporation of 1 mol of tightly bound *Eco*-ES_7 and 6−6.5 mol of tightly bound ADP per mol of complex (Table 3). These asymmetric *Tbr*-EL_{14}·*Tbr*-ES_7 and *Tbr*-EL_{14}·*Eco*-ES_7 complexes are similar to that isolated from *T. thermophilus* (Taguchi et al., 1991) or that formed using *E. coli* chaperonins (Todd et al., 1993).

The formation of the tetradecamer complex was rapid, occurring before one site equivalent of ATP could turn over. This result, plus the ability to dimerize upon addition of the ATP analog AMP-PNP, was consistent with the mechanism proposed in Scheme 1. *Tbr*-EL_7 binds nucleotide, followed by rapid binding of *Eco*-ES_7 to produce a *Tbr*-EL_7 toroid ("half-football") committed to dimerize. There is precedent for rapid interaction between the rings of GroES and GroEL. Such interaction depends upon the prior binding of nucleotide to GroEL. For example, *Eco*-ES_7 binds to one of the two rings of the binary *Eco*-EL_{14}·ATP_n complex at rates approaching the diffusional limit (>4 × 10^7 M^{-1} s^{-1}) (Burston et al., 1995). There is also precedent for the existence of complexes containing a single ring of $GroEL_7$ and $GroES_7$. Electron micrographs of such "half-footballs" containing one ring each of *Tth*-EL_7 and *Tth*-ES_7 have been reported (Ishii et al., 1995). This fully ligated toroid could potentially dimerize with another fully ligated toroid (Scheme 1, path A) or with an unligated toroid (Scheme 1, path B) to produce the stable *Tbr*-EL_{14}·$GroES_7$ complex.

Scheme 1 path A involves the transient formation of a symmetrical complex, equivalent to the "football-shaped" species that was observed both with *E. coli* chaperonins (Azem et al., 1994b; Schmidt et al., 1994b; Llorca et al., 1994; Harris et al., 1994) and with *T. thermophilus* chaperonins (Taguchi et al., 1991; Ishii et al., 1995) which we have proposed is an intermediate in the chaperonin cycle (Todd et al., 1994). While our experimental observations are consistent with path A, they do not formally exclude path B. However, Ishii et al. (1995) have reported that the chaperonin complex from *T. thermophilus*, *Tth*-EL_{14}·ADP_7·*Tth*-ES_7, undergoes an equatorial split in the presence of ATP and K^+ into a 7-mer complex that is thought to correspond to a *Tth*-EL_7·ANP_7·*Tth*-ES_7 or "half football". Since this equatorial dissociation was stimulated by the addition of excess *Tth*-ES_7, it was suggested that the reaction proceeded via a symmetrical, "football-shaped" *Tth*-ES_7·ANP_7·*Tth*-EL_{14}·ATP_7·*Tth*-ES_7 complex. The dissociative reaction they describe thus appears to be the reverse of the associative reaction that we have observed (i.e., Scheme 1, path A). Ishii et al. (1995) used low concentrations of Mg^{2+} in their dissociative experiments, whereas we have employed much higher concentrations of Mg^{2+} in our associative experiments. We suggest that Ishii et al. (1995) and we are observing the same reaction, in opposite directions.

Although we cannot presently exclude the possibility that a singly toroidal chaperonin assists protein folding, the experimental evidence argues against this. *Eco*-EL_{14} facilitates the folding of some proteins in the absence of *Eco*-ES_7, especially under conditions that are at least partly permissive for folding (Laminet et al., 1990; Viitanen et al., 1991; Schmidt et al., 1994a). It was therefore to be expected that *Tbr*-EL_7 might undertake those partial reactions for which there is no obligate requirement for GroES. Indeed, the singly toroidal *Tbr*-EL_7 could bind unfolded protein, suppress aggregation (Figures 5 and 6), hydrolyze ATP (Figure 3), and release unfolded Rubisco upon ATP hydrolysis (M.J.T., unpublished results). Thus we predict that under permissive folding conditions *Tbr*-EL_7 should enhance the folding of those proteins which do not require GroES. Under nonpermissive conditions, however, *Tbr*-EL_7 failed to support folding in the absence of GroES. Of course, the presence of GroES and ATP are the very conditions which lead to rapid dimerization of *Tbr*-EL_7 and the formation of the asymmetric and symmetric complexes believed to be intermediates in the productive folding cycle (Todd et al., 1994).

Significantly, the isolated *Tbr*-EL_{14}·ADP_7·*Tbr*-ES_7 was unable to fold Rubisco in the absence of additional *Eco*-ES_7 (Figure 5); the molar equivalent of *Tbr*-ES_7 which copurified with *Tbr*-EL_{14} was not sufficient to support the protein folding reaction. This is consistent with a reaction mechanism requiring more than one mole $GroES_7$ per $GroEL_{14}$ during the chaperonin protein folding cycle (Todd et al., 1994).

Substoichiometric binding of unfolded protein to *Tbr*-EL_7 and *Tbr*-EL_{14}·*Tbr*-ES_7 demonstrated that the doubly toroidal chaperonin bound unfolded Rubisco with ~2-fold higher affinity. Stoichiometric binding of nearly 1 mol of unfolded Rubisco per mol of *Tbr*-EL_7 or *Tbr*-EL_{14}·*Tbr*-ES_7 was demonstrated using an excess of Rubisco to toroids (Table 5). Surprisingly, *Eco*-EL_{14} could simultaneously (and stably) bind almost *2* mol of unfolded protein, confirming that double toroids contain two protein binding sites. Several previous experiments have been consistent with two unfolded proteins bound to GroEL (Viitanen et al., 1991; Bochkareva et al., 1992). However, others have only been able to observe a single bound polypeptide (Laminet et al., 1990; Martin et al., 1991). On the basis of the proposed reaction mechanism for *Eco*-EL (Todd et al., 1994), a given molecule may only have one high affinity site available during the protein folding reaction. Thus while static binding of two moles protein can be observed, only one toroid may be assisting in the protein folding reaction at a given instant.

Formation of the asymmetric complexes with both *T. brockii* and *E. coli* chaperonins confirmed that when one toroid was occupied by $GroES_7$, one of the two binding sites for unfolded protein was sterically blocked. However, when an *Eco*-EL_{14} with two unfolded proteins bound was converted to the asymmetric complex, significantly greater than one unfolded protein remained bound (Table 5). This result was consistent with a stable chaperonin complex now containing one unfolded protein opposite the GroES and another on the same GroEL toroid as GroES. We note that previous localization of unfolded protein bound to the asymmetric complex detected additional electron dense mass (Chen et al., 1994) or substrate protein antigen (Ishii et al., 1994) only on the toroid opposite the co-chaperonin. However, as we show here, the order of addition of the two ligands, GroES and unfolded substrate protein, influences the composition and stoichiometry of the final ternary complex. The simultaneous binding of more than one unfolded protein leads to a question of where in the chaperonin cycle the unfolded substrate protein is released. We have previously demonstrated that unfolded protein bound opposite co-chaperonin is rapidly released upon addition of ADP (Todd et al., 1994). Our results in Table 5 are in agreement, but suggest that additional unfolded protein (bound under the GroES cap) cannot be released with ADP. Since this complex becomes committed to dissociate upon binding ATP (Todd et al., 1994), the following mechanism for chaperonin folding is proposed: (1) Unfolded protein binds tightly, opposite the GroES. (2) One revolution around the GroEL ATPase cycle would involve ATP and GroES binding on top of this unfolded protein substrate and, following ATP hydrolysis, may result in a peptide trapped beneath the GroES. (3) A second revolution around the cycle would release the unfolded protein, which (4) could repartition between native and misfolded structures.

This hypothesis is consistent with release of unfolded protein only occurring upon ATP hydrolysis at the GroEL toroid opposite an unfolded protein, releasing GroES, ADP, and the unfolded protein, all from the same toroid. It is also consistent with $t_{1/2}$ of release being 20−30 s (Todd et al., 1994; Weissman et al., 1994) or equal to once for every two revolutions around the ATPase cycle. Further experiments are currently underway to evaluate this mechanism.

REFERENCES

Azem, A., Diamant, S., & Goloubinoff, P. (1994a) *Biochemistry 33*, 6671−6675.

Azem, A., Kessel, M., & Goloubinoff, P. (1994b) *Science 265*, 653−656.

Braig, K., Otwinowski, Z., Hegde, R., Boisvert, D. C., Joachimiak, A., Horwich, A. L., & Sigler, P. B. (1994) *Nature 371*, 578−586.

Bochkareva, E. S., & Girshovich, A. S. (1992) *J. Biol. Chem. 267*, 25672−25675.
Bochkareva, E. S., Lissin, N. M., Flynn, G. C., Rothman, J. E., & Girshovich, A. S. (1992) *J. Biol. Chem. 267*, 6796−6800.
Buchner, J., Schmidt, M., Fuchs, M., Jaenicke, R., Rudolph, R., Schmid, F. X., & Kiefhaber, T. (1991) *Biochemistry 30*, 1586−1591.
Burston, S. G., Ranson, N. A., & Clarke, A. R. (1995) *J. Mol. Biol. 249*, 138−152.
Chen, S., Roseman, A. M., Hunter, A. S., Wood, S. P., Burston, S. G., Ranson, N. A., Clarke, A. R., & Saibil, H. R. (1994) *Nature 371*, 261−264.
Goloubinoff, P., Christeller, J. T., Gatenby, A. A., & Lorimer, G. H. (1989) *Nature 342*, 884−889.
Gray, T. E., & Fersht, A. R. (1991) *FEBS Lett. 292*, 254−258.
Harris, J. R., Plückthun, A., & Zahn, R. (1994) *J. Struct. Biol. 112*, 216−230.
Hayer-Hartl, M. K., & Hartl, F. U. (1993) *FEBS Lett. 320*, 83−84.
Hendrix, R. W. (1979) *J. Mol. Biol. 129*, 375−392.
Ishii, N., Taguchi, H., Sasabe, H., & Yoshida, M. (1994) *J. Mol. Biol 236*, 691−696.
Ishii, N., Taguchi, H., Sasabe, H., & Yoshida, M. (1995) *FEBS Lett. 362*, 121−125.
Laminet, A. A., Ziegelhofer, T., Georgopoulos, C., & Plückthun, A. (1990) *EMBO J. 9*, 2315−2319.
Langer, T., Pfeifer, G., Martin, J., Baumeister, W., & Hartl, F.-U. (1992) *EMBO J. 11*, 4757−4765.
Llorca, O., Marco, S., Carrascosa, J. L., & Valpuesta, J. M. (1994) *FEBS Lett. 345*, 181−186.
Martin, J., Langer, T., Boteva, R., Schramel, A., Horowich, A. L., & Hartl, F.-U. (1991) *Nature 352*, 36−42.
McMullin, T. W., & Hallberg, R. L. (1988) *Mol. Cell. Biol. 8*, 371−380.
Mendoza, J. A., Demeler, B., & Horowitz, P. M. (1994) *J. Biol. Chem. 269*, 2447−2451.
Miller, S. G., Leclerc, R. F., & Erdos, G. W. (1990) *J. Mol. Biol. 214*, 407−422.
Musgrove, J. E., Johnson, R. A., & Ellis, R. J. (1987) *Eur. J. Biochem. 163*, 529−534.
Pushkin, A. V., Tsuprun, V. L., Solovjeva, N. A., Shubin, V. V., Evistigneeva, Z. G., & Kretovich, W. L. (1982) *Biochim. Biophys. Acta 704*, 379−384.
Saibil, H. R., Zeng, D., Wood, S. P., & auf der Mauer, A. (1991) *Nature 353*, 25−26.
Schmidt, M., Buchner, J., Todd, M. J., Lorimer, G. H., & Viitanen, P. V. (1994a) *J. Biol. Chem. 269*, 10304−10311.
Schmidt, M., Rutkat, K., Rachel, R., Pfeifer, G., Jaenicke, R., Viitanen, P. V., Lorimer, G. H., & Buchner, J. (1994b) *Science 265*, 656−659.
Taguchi, H., Konishi, J., Ishii, N., & Yoshida, M. (1991) *J. Biol. Chem. 266*, 22411−22418.
Todd, M. J., Viitanen, P. V., & Lorimer, G. H. (1993) *Biochemistry 32*, 8560−8567.
Todd, M. J., Viitanen, P. V., & Lorimer, G. H. (1994) *Science 265*, 659−666.
Truscott, W. N., Høj, P. B., & Scopes, R. K. (1994) *Eur. J. Biochem. 222*, 277−284.
van der Vies, S. M., Viitanen, P. V., Gatenby, A. A., Lorimer, G. H., & Jaenicke, R. (1992) *Biochemistry 31*, 3635−3644.
Viitanen, P. V., Lubben, T. H., Reed, J., Goloubinoff, P., O'Keefe, D. P., & Lorimer, G. H. (1990) *Biochemistry 29*, 5665−5671.
Viitanen, P. V., Donaldson, G. K., Lorimer, G. H., Lubben, T. H., & Gatenby, A. A. (1991) *Biochemistry 30*, 9716−9723.
Viitanen, P. V., Lorimer, G. H., Seetharam, R., Gupta, R. S., Oppenheim, J., Thomas, J. O., & Cowan, N. J. (1992) *J. Biol. Chem. 267*, 695−698.
Weismann, J. S., Kashi, Y., Fenton, W. A., & Horwich, A. R. (1994) *Cell 78*, 693−702.

BI9512197